



Design, implementation and production upscaling of novel, high-performance, cluster-based catalysts for CO₂ hydrogenation

Deliverable D.2.2

First report on the in situ characterization of cluster-based ECs



Grant Agreement No:	955650
Project start date:	01.11.2020
Duration of the project:	48 months
Deliverable number	2.2
Deliverable leader	PSI/KUL
Due date:	31/10/2022 (M48)
Actual submission date:	07/12/2022
Dissemination level:	CO
Author(s):	Maximilian Winzely, Joao Coroa

Contents

Goal.....	3
1. Approach.....	3
2. Results.....	4
2.1. <i>In situ</i> XAFS of a 50 $\mu\text{g}_{\text{Pd}}/\text{cm}^2$ electrode.....	4
Linear Combination Fitting (LCF).....	4
Extended X-Ray Absorption Fine Structure (EXAFS) Analysis.....	4
2.2. <i>In situ</i> XAFS of a Pd cluster-based EC with 5 $\mu\text{g}_{\text{Pd}}/\text{cm}^2$	5
Electrochemical Surface Area (ECSA).....	5
In situ XAFS.....	5
3. Experimental details.....	6
3.1. Preparation of the electrodes.....	6
Pd commercial nanoparticles (50 $\mu\text{g}_{\text{Pd}}/\text{cm}^2$).....	6
Pd gas-phase clusters (5 $\mu\text{g}_{\text{Pd}}/\text{cm}^2$).....	6
3.2. Electrochemistry.....	7
3.3. <i>In situ</i> XAFS.....	7
4. Conclusions.....	7
5. References.....	8

Deliverable D.2.2 First report on the in situ characterization of cluster-based ECs**Goal.**

The final goal is to use *operando* X-Ray absorption fine structure spectroscopy (XAFS) to investigate a cluster-based electrode under carbon dioxide reduction reaction (CO₂RR) conditions in a *newly designed* electrochemical flow cell.

1. Approach.

We used a spectroelectrochemical flow cell (depicted in Fig. 1) designed by ESR 14 (Maximilian Winzely) that enables spectral acquisition in fluorescence mode using an X-ray beam incidence angle of $\leq 0.1^\circ$ with regards to the working electrode substrate plane (i.e., in a so called grazing incidence (GI) configuration). This special geometry allows maximizing the interaction length of the X-ray beam with the clusters deposited at the electrode substrate using Cluster Beam Deposition with typical metal loadings below $10 \mu\text{g}_{\text{metal}}/\text{cm}_{\text{geom}}^2$.

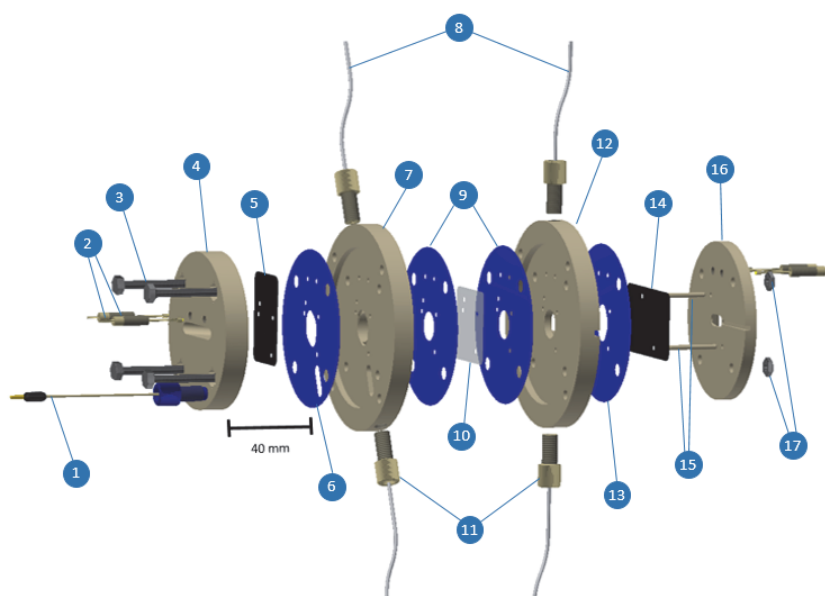


Figure 1 Technical drawing of the GIXAS cell assembly consisting of a leak-free Ag/AgCl reference electrode (1), four gold contact pins (2), four M4 screws (3), outer counter electrode part (4), counter electrode (5), counter electrode gasket (6), inner counter electrode part (7), tubing for electrolyte (8), two membrane gaskets (9), a Nafion® XL membrane (10), PEEK screws (11), inner working electrode part (12), working electrode gasket (13), Kapton® foil with carbon layer and catalyst (14), alignment pins (15), outer working electrode part (16), and nuts (17)

To test the functionality of the cell two types of palladium (Pd) samples were prepared to study the formation of palladium hydride (PdH_x) as a function of the applied potential in an argon-saturated phosphate buffer electrolyte.[1] A commercial 20 % Pd/C catalyst was drop-casted onto the working electrode substrate to produce an electrode with a loading of $50 \mu\text{g}_{\text{Pd}}/\text{cm}^2$. This sample was used to investigate the transient effect of the studied reaction and point out the high time resolution of the novel *in situ* GIXAS cell for thin layer electrodes. Additionally, a second sample provided by ESR 2 (Joao Corao) at TCL consisting of monodispersed Pd-clusters deposited using a magnetron CBD source on the electrode substrate with a loading of $5 \mu\text{g}_{\text{Pd}}/\text{cm}^2$ was studied as an example of low loaded catalyst still measurable within one hour.

2. Results.

2.1. *In situ* XAFS of a 50 $\mu\text{g}_{\text{Pd}}/\text{cm}^2$ electrode

Linear Combination Fitting (LCF)

As mentioned earlier, the higher loaded, Pd/C sample was used to study the formation of PdH_x using LCF, which demonstrates the remarkable high time-resolution of the flow cell for thin film electrodes. For this purpose, two XA spectra were recorded every second during 10-minute holds at 11 different potentials between -0.1 and 0.5 V vs. the reversible hydrogen electrode (RHE). Twenty of these time-resolved spectra were averaged and LC-fitted in the next step with two standards recorded for the same electrode in the metallic (recorded at 0.5 V vs. RHE in 0.1 M) and full hydride states (recorded at 0.5 or -0.1 V vs. RHE in Ar-saturated phosphate buffer electrolyte, respectively – see Fig. 2).

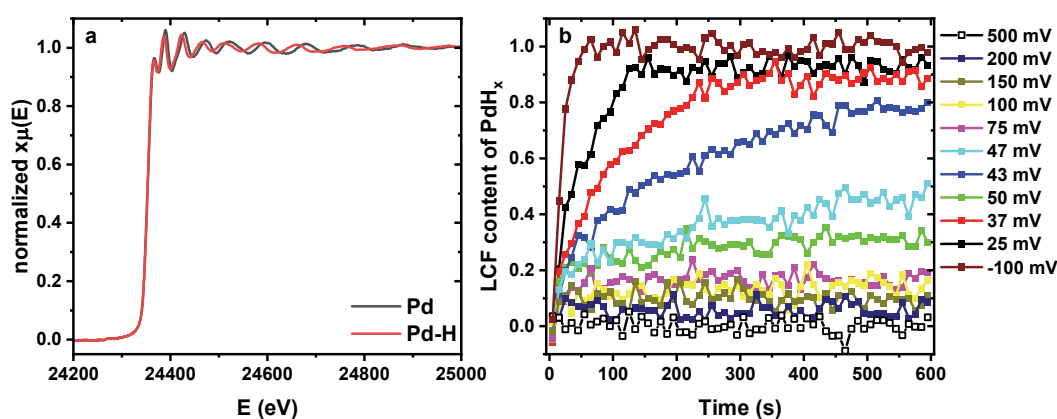


Figure 2 (a) Normalized in-situ XA-spectra at the Pd K-edge of a 20 % Pd/C electrode with a loading of 50 $\mu\text{g}_{\text{Pd}}/\text{cm}^2$ at 0.5 or -0.1 V vs. RHE (corresponding to metallic Pd vs. fully stoichiometric Pd-hydride, respectively) that were used as references for the linear combination fits of the spectra for tracking the time-dependent formation of PdH_x at varying potential holds shown in (b). All measurements were recorded in Ar-saturated 0.1 M $\text{KH}_2\text{PO}_4/\text{K}_2\text{HPO}_4$ ($\text{pH} \approx 6.8$) using the newly designed operando GIXAS cell. Note that the potentials in (b) are quoted against the RHE scale.

Extended X-Ray Absorption Fine Structure (EXAFS) Analysis

In addition, EXAFS analysis was performed to determine the Pd-Pd bond distance and the corresponding Pd-hydride-stoichiometry (i.e., the 'x' in PdH_x) at equilibrium at each potential. Therefore, the bond distance was converted to x of the PdH_x stoichiometry according to equation[2]:

$$\frac{\Delta R(T)}{R_0(T)} = 0.0666x - 0.0164x^2$$

where $R_0(T)$ is defined as the Pd-Pd bond distance in the metallic state and $\Delta R(T)$ as the deviation from the latter at the given temperature. In Figure 3a, these results are compared to those inferred from

the electrochemical hydride oxidation charges determined from a positive going linear sweep after each potential hold (see Fig. 3b). For the EXAFS fit, the last three minutes of the XAFS-spectra at each potential were averaged, explaining the slightly lower x values obtained at intermediate potentials compared to those derived from the electrochemical hydride oxidation charges.

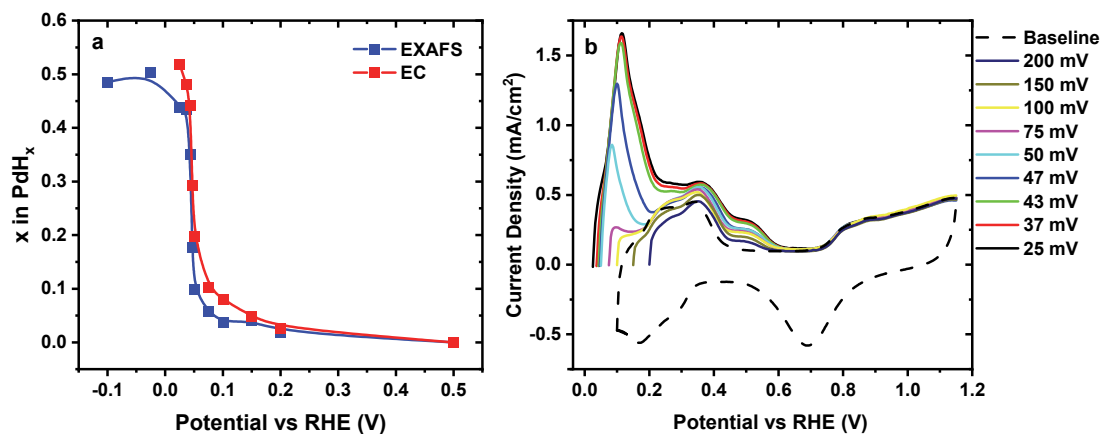


Figure 3 (a) PdH_x stoichiometry determined from the EXAFS-fitted Pd-Pd bonding distance and hydride oxidation charges when the potential was held for 10 min at values between 0.5 and -0.1 V vs. RHE and (b) positive going linear sweeps after the same potential holds, including a cyclic voltammogram used as a baseline to determine the hydride oxidation charges. All CVs were recorded at a scan rate of 20 mV/s in N_2 -saturated 0.1 M phosphate buffer on a Pd/C electrode with a loading of $50 \mu\text{g}_{\text{Pd}}/\text{cm}^2$

2.2. *In situ* XAFS of a Pd cluster-based EC with $5 \mu\text{g}_{\text{Pd}}/\text{cm}^2$

Electrochemical Surface Area (ECSA)

The ECSA of the cluster-based catalyst sample was determined from hydrogen under potential deposition to be $\approx 50\%$ of the geometric area of the working electrode. This may be due to some level of agglomeration of the clusters occurring during their deposition and leading to the possible formation of palladium cluster islands. Further optimization of the deposition conditions may be required to minimize this effect.

In situ XAFS

This sample was used to demonstrate that even with this small amount of Pd, an *in situ* XAFS spectrum can be recorded within one hour using the novel flow cell. In detail, the electrode was polarized to 0.5 V and -0.1 V vs RHE to record a spectrum in the metallic and full hydride state, respectively.

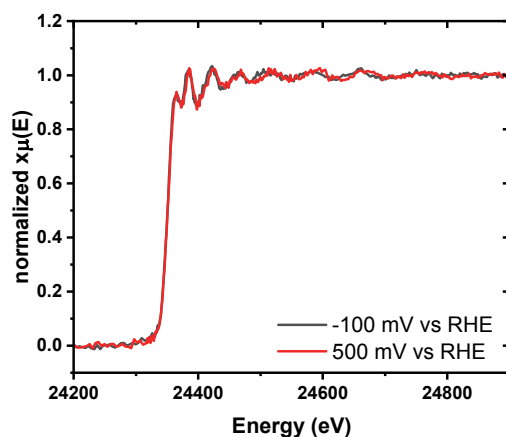


Figure 4 Normalized, *in situ* XAFS spectra at the Pd K-edge of the sample prepared by ESR 2 with a loading of 5 $\mu\text{g}_{\text{Pd}}/\text{cm}^2$ at 0.5 or -0.1 V vs. RHE (corresponding to metallic vs. fully stoichiometric Pd-hydride, respectively)

3. Experimental details.

3.1. Preparation of the electrodes

Pd commercial nanoparticles ($50 \mu\text{g}_{\text{Pd}}/\text{cm}^2$)

For the preparation of this electrode, a catalyst consisting of Pd nanoparticles supported on a carbon black (Vulcan XC-72) commercially available from Premetek (P30A200) was used. For drop-casting the catalyst onto the working electrode substrate (Electrically conductive Kapton® 200RS100) an ink was prepared by weighing ≈ 5 mg of catalyst powder into a vial and dispersing it in ultrapure water ($18.2 \text{ M}\Omega\cdot\text{cm}$, ELGA Purelab Ultra) and isopropanol (Sigma-Aldrich, HPLC grade, 99.9%) using a volume ratio of 9 to 1. Additionally, Nafion™ perfluorinated resin (Sigma-Aldrich, 5%) was added as a binder where the amount was selected to yield a Nafion to carbon mass ratio of 0.2. In the next step, the ink was ultra-sonicated for at least 20 minutes. The total volume of ink was chosen to achieve the desired loading of $50 \mu\text{g}_{\text{Pd}}/\text{cm}^2$ with a droplet volume of $50 \mu\text{L}$. To drop-cast the catalyst in the desired shape (i.e., a circle with a diameter of 10 mm) and position, a mask similar to the one described by Diercks *et al.*[3] was used.

Pd gas-phase clusters ($5 \mu\text{g}_{\text{Pd}}/\text{cm}^2$)

This electrode was prepared by ESR 2 using magnetron sputtering cluster beam deposition. This technique has the advantage of producing clusters without any chemicals or ligands that might reduce the activity of the cluster-based catalyst. However, it typically features limited throughput as indicated by the low loading ($5 \mu\text{g}_{\text{Pd}}/\text{cm}^2$) when compared with the above electrode ($50 \mu\text{g}_{\text{Pd}}/\text{cm}^2$). A 2-inch Pd target with 99.5% purity was used to produce the clusters and the electrode substrate was the same electrically conductive Kapton® 200RS100. The starting sputtering power was 15 W and after stabilization, 295 V were being given to the electrons to ionize the Ar atoms. Pd clusters were grown at an aggregation length of 30 cm, 0.48 mbar with 135 sccm of Ar and 15 sccm of He and at a surrounding condensation chamber cooled by liquid nitrogen. The cluster beam was bent by a 90° angle through a set of optical lenses and deposited at the substrate biased with 900 V. The current measured at the substrate, which represents the cluster deposition process, was on average 16 nA and the total deposition time was 4 minutes.

3.2. Electrochemistry

The 0.1 M phosphate buffer was prepared by dissolving 2.041 g di-potassium hydrogen phosphate (K_2HPO_4 , Merck LiChropur, anhydrous, 99.999%) and 1.808 g potassium dihydrogen phosphate (KH_2PO_4 , Merck, LiChropur, anhydrous, 99.999%) in 250 mL of ultrapure water resulting in a pH close to 6.8. The Ag/AgCl reference electrode was calibrated in the same electrolyte (saturated with H_2) by performing a hydrogen oxidation/evolution experiment on a polycrystalline platinum rotating disk electrode at 1600 rpm.

Following the deaeration of the electrolyte for at least 30 minutes with argon (4.6), the cell was filled with electrolyte at a flow rate of 0.5 mL/min through PEEK lines connected to the bottom of the cell and the electrolyte container. Once the working and counter compartments were fully filled, the flow was lowered to 0.05 mL/min and the alignment of the cell was performed until the highest fluorescence signal was obtained. Simultaneously, an electrochemical impedance spectrum was recorded at the open circuit voltage with a perturbation of 10 mV to determine the high frequency resistance, so that the potential could be corrected for 85 % of its value in all the following measurements.

3.3. *In situ* XAFS

The *in situ* XAFS experiments were performed at the Super-XAS beamline (X10DA) of the Swiss Light Source (SLS). During the potential holds XAFS-spectra were acquired at the Pd K-edge (24.350 keV) in fluorescence mode. The polychromatic beam was generated by a 2.9 T superbend magnetic source and was collimated by a Pt-coated mirror at 2.84 mrad. The monochromatic beam was produced by a Si(111) channel-cut quick-scanning monochromator with liquid N_2 cooling. The beam was focused to a spot size of $0.15 \times 0.15 \text{ mm}^2$ with a Pt-coated toroidal mirror. The beam flux interacting with the sample was determined to be 5×10^{10} photons/s. Three identical ionization chambers (15 cm length, filled with Ar 0.5 bar and N_2 0.5 bar) were used to measure the incident beam intensity as a function of energy (before the sample) and the XAS signal from Pd-foil placed in front of a third ionization chamber, for absolute energy calibration of every acquired sample spectrum. For the higher loaded sample ($50 \mu\text{g}_{Pd}/\text{cm}^2$) fluorescence detection was performed in quick XAS mode using QuickXAS (with a PIPS diode detector from Mirion Technology) during monochromator oscillation with 1 Hz frequency. In the case of the $5 \mu\text{g}_{Pd}/\text{cm}^2$ sample, the Pd K-edge spectra were acquired in a step-by-step mode with a silicon drifts detector (SDD) comprising of 5 elements (450 μm thickness) from SGX. To align the working cell with the sample in the grazing incidence geometry, the vertical, horizontal, and angle-dependent scans were performed sequentially with respect to the beam in an iterative procedure until the highest Pd $K\alpha$ fluorescence signal was recorded at the SDD detector, for all samples.

4. Conclusions.

A newly designed spectro-electrochemical flow cell has been successfully tested for its ability to track electrochemical processes in the seconds range when a thin layer electrode is used. This brings advantages such as better mass transport behavior, better potential distribution and less delamination of the catalyst layer.[4]

In addition, it has been shown that with very small amounts of catalyst, as in the case of cluster-based electrodes, an XAFS spectrum can be recorded from the steady state of the material within one hour.

Further improvements will be made to reduce the agglomeration of the clusters during their deposition and increase the roughness factor of the electrode substrate.

5. References

1. Diercks, J.S., et al., *Interplay between Surface-Adsorbed CO and Bulk Pd Hydride under CO₂-Electroreduction Conditions*. ACS Catalysis, 2022: p. 10727-10741.
2. Siebel, A., et al., *Identification of Catalyst Structure during the Hydrogen Oxidation Reaction in an Operating PEM Fuel Cell*. ACS Catalysis, 2016. **6**(11): p. 7326-7334.
3. Diercks, J.S., et al., *An Online Gas Chromatography Cell Setup for Accurate CO₂-Electroreduction Product Quantification*. Journal of The Electrochemical Society, 2021. **168** 064504.
4. Diklić, N., et al., *Potential Pitfalls in the Operando XAS Study of Oxygen Evolution Electrocatalysts*. ACS Energy Letters, 2022. **7**(5): p. 1735-1740.